EPJ Web of Conferences **279**, 11010 (2023) https://doi.org/10.1051/epjconf/202327911010
NPA-X 2022

Indirect measurement of the $(n,\gamma)^{127}$Sb cross section

Francesco Pogliano[1,*], *Ann-Cecilie* Larsen[1,**], *Frank Leonel* Bello Garrote[1], *Marianne* Møller Bjørøen[1], *Thomas* Kvalheim Eriksen[1], *Dorthea* Gjestvang[1], *Andreas* Görgen[1], *Magne* Guttormsen[1], *Kevin Ching Wei* Li[1], *Maria* Markova[1], *Eric Francis* Matthews[2], *Wanja* Paulsen[1], *Line* Gaard Pedersen[1], *Sunniva* Siem[1], *Tellef* Storebakken[1], *Tamás* Gabor Tornyi[1], and *Julian* Ersland Vevik[1]

[1]Department of Physics, University of Oslo, N-0316 Oslo, Norway
[2]Department of Nuclear Engineering, University of California, Berkeley, California 94720 U.S.A.

Abstract. Sensitivity studies of the *i* process have identified the region around ^{135}I as a bottleneck for the neutron capture flow. Nuclear properties such as the Maxwellian-averaged cross section (MACS) are key to constrain the uncertainties in the final abundance patterns. With the Oslo method, we are able to indirectly measure such properties for the nuclei involved in this process. From the ^{124}Sn$(\alpha, p\gamma)^{127}$Sb reaction data we extract the nuclear level density and γ-ray strength function for ^{127}Sb. The level density at higher excitation energies is compatible with the constant-temperature model, while the γ-ray strength function presents features like an upbend and a pygmy-like structure below S_n. From these two quantities we can calculate the MACS for the ^{126}Sb$(n,\gamma)^{127}$Sb reaction using the Hauser-Feshbach formalism, and constrain its uncerainties from the theoretical ones. Libraries such as JINA REACLIB, TENDL and BRUSLIB agree well with the experimental results, while ENDF/B-VIII.0 predicts a higher rate.

1 Introduction

Burbidge et al. [1] in 1957 in their seminal paper identified the *s* and the *r* processes (standing for the slow and rapid neutron-capture processes, respectively) as the main mechanisms behind the creation of the elements heavier than iron in our universe. The two nucleosynthesis processes produce different elemental abundance patterns, and while our Sun's abundance presents characteristics from both processes, in many stars only the pattern from one of these may be observable [2]. This is the case for carbon-enhanced, metal-poor stars (CEMPs), which may be enriched in *r* process elements [3], *s* process elements or both [4]. This last case is challenging to explain, as the two nucleosynthesis processes are thought to happen in different astrophysical sites, and CEMPs are thought to have formed before the interstellar medium from them could mix. A possible solution to this problem is the introduction of the *i* process. The *i* process stands for intermediate neutron-capture process, has neutron densities between those of the *s* and the *r* process, and was first proposed in 1977 by Cowan and Rose [5]. Sensitivity simulations of this process are able to reproduce the abundances for

*e-mail: francesco.pogliano@fys.uio.no
**e-mail: a.c.larsen@fys.uio.no

these CEMPs-s/r (CEMPs presenting elements characteristics to both the *s* and *r* process), and identify the region around ^{135}I as a bottleneck [6]. However, one of the main sources of uncertainty lies in the correct estimation of nuclear properties such as the neutron-capture rates of the nuclei involved in the *i* process. By carrying out experimental studies in the ^{135}I region we are able to constrain uncertainties for the neutron-capture rates. This also provides useful experimental measurements of nuclear properties so that better and more precise theoretical models may be developed, these being very important for both *i* and *r* process simulations. This region of the nuclear chart involves many unstable, neutron-rich nuclei, for whose it is very difficult to carry direct measurements of the (n, γ) reaction cross section. For this reason an indirect approach is used. With the Oslo method we are able to extract two statistical properties of the nucleus, the nuclear level density (NLD) and the γ-ray strength function (GSF). The NLD and GSF are statistical properties of the nucleus, the first one being the "continuous" equivalent of counting energy levels, and the second of the reduced transition probabilities. These are the ingredients needed in the Hauser-Feshbach formalism (together with the optic model potential) to calculate the neutron-capture rate (see [7] and references therein.) Here we present the results from the ^{124}Sn$(\alpha, p\gamma)^{127}$Sb experiment. By analyzing the data with the Oslo method we obtain the NLD and the GSF of ^{127}Sb, part of the ^{135}I region. The $(n, \gamma)^{127}$Sb reaction rate is then calculated, presented and compared to known libraries.

2 The extraction of the NLD and GSF

The ^{124}Sn$(\alpha, p\gamma)^{127}$Sb reaction experiment was carried out at the Oslo Cyclotron Laboratory for a period of five days. a 24 MeV α-beam was impinged on a self-supporting ^{124}Sn target. In order to use the Oslo method, we are interested in particle-γ coincidences. For this reason the reaction data was collected using a silicon particle detector (SiRi [8],) and a $LaBr_3$ γ-ray detector (OSCAR, [9]). The particle detector consists of a thin front detector (ΔE) and a thicker back detector (E), and this allows us to separate the different reaction channels and only select the (α, p) data. From the energy of the beam and that of the ejected proton, we are able to calculate the excitation energy the resulting ^{127}Sb is left in, and associate it to the coinciding γ-rays from its de-excitation to the ground state. These different γ-ray spectra for each excitation energy can be plotted together in a matrix, called raw coincidence matrix. The Oslo method is a procedure for which we can obtain the NLD and the GSF of a nucleus starting from a raw coincidence matrix [10–12]. First the matrix has to be unfolded to get rid of the detector response. Secondly, The first-generation matrix is obtained with a subtraction technique, where we only select the first γ-rays from each de-excitation. The NLD and the GSF are used to describe the nucleus in the quasicontinuum excitation energy region, where the level density becomes so large ($\gtrsim$ 50 per MeV) that it is more useful to describe nuclear properties statistically. These are then extracted from the first-generation matrix from this region using a χ^2 minimization algorithm explained in Ref. [12] and finally normalized following the procedure described in the main article about this experiment (Ref. [13]). The extracted NLD and GSF are shown in Figure 1. Here we see how the NLD follows an exponential curve compatible with the constant-temperature model. The GSF shows features such as the upbend at low energies, the pygmy resonance and possibly a small structure at $\approx$ 3 MeV. For each graph, all the available TALYS 1.95 [15, 16] models were plotted as comparison, showing a general disagreement to the experimental data.

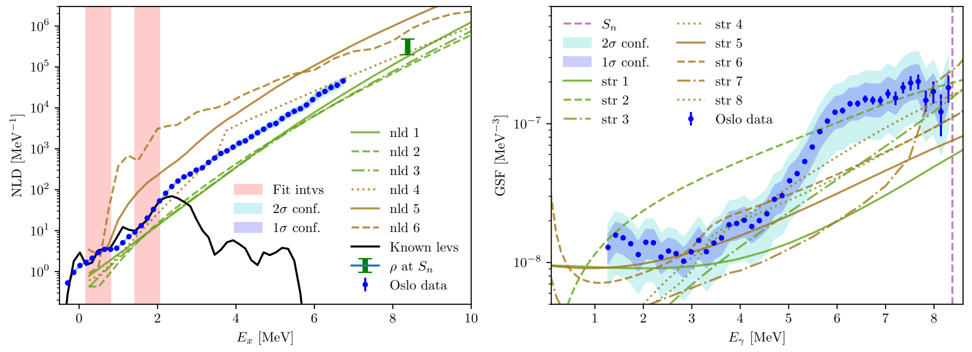

Figure 1. The NLD (left) and the GSF (right) for ^{127}Sb. `nld` and `str` indicate the model number obtained from TALYS 1.95 [15, 16]. The red bars in the left plot indicate the low excitation energy regions the NLD was normalized to (see Ref. [13] for details.)

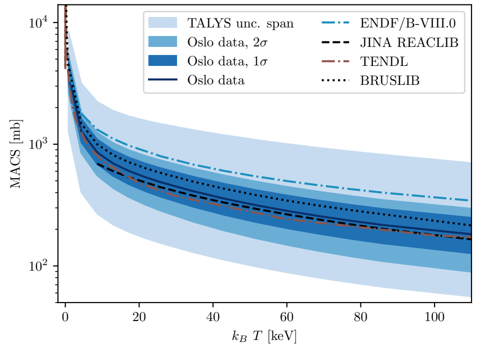

Figure 2. The constrained MACS uncertainty for the $(n,\gamma)^{127}$Sb reaction, compared to the uncertainty range from combining all the NLD and GSF theoretical models from TALYS.

3 The MACS

The Maxwellian-averaged cross section (MACS) is a quantity easily translatable to the neutron-capture rate [14] and is an important nuclear input parameter for nucleosynthesis simulations. Theoretical MACSs can be calculated with TALYS in the Hauser-Feshbach framework by choosing a NLD, a GSF and a optical model potential. While the latter does not influence the MACS too much, combining all the models gives an uncertainty span of more than one order of magnitude (see Figure 2). The experiment data constrains this uncertainty and is compared to common libraries such as JINA REACLIB [17], BRUSLIB [18], TENDL [16] and ENDF/B-VIII.0 [19]. While the first three give predictions within 1σ uncertainty from the experimental result, the latter predicts values outside the 2σ uncertainty region.

References

[1] M. Burbidge et al., Rev. Mod. Phys. **29**, 547 (1957)
[2] M. Arnould et al., Physics Reports **450**, Pages 97-213 (2007)
[3] T. Hansen et al., ApJ **807**, 173 (2015)
[4] C. Sneden et al., Ann. Rev. of A&A **46:1**, 241-288 (2008)

[5] J. J. Cowan et al., ApJ **212**, 149-158 (1977)
[6] M. Hampel et al., ApJ **831**, 171 (2016)
[7] A.C. Larsen et al., PPNP **107**, Pages 69-108 (2019)
[8] M. Guttormsen et al., Nucl. Instrum. Methods Phys. Res. Sect. A **648**, 168 (2011)
[9] F. Zeiser et al., Nucl. Instrum. Methods Phys. Res. Sect. A **985**, 164678 (2020)
[10] M. Guttormsen et al., Nucl. Instrum. Methods Phys. Res. Sect. A **374**, 371 (1996)
[11] M. Guttormsen et al., Nucl. Instrum. Methods Phys. Res. Sect. A **255**, 518 (1987)
[12] A. Schiller et al., Nucl. Instrum. Methods Phys. Res. Sect. A **447**, 498 (2000)
[13] F. Pogliano et al. Phys. Rev. C **106**, 015804 (2022)
[14] C. Iliadis, N*uclear Physics of Stars* (Wiley-VCH, Weinheim, 2015) 147-150
[15] A. Koning et al., User manual, Tech. Rep., (2017)
[16] A. Koning et al., Nucl. Data Sheets **155**, 1 (2019)
[17] R. H. Cyburt et al., ApJ Suppl. Series **189**, 240 (2010)
[18] Y. Xu et al., Astron. Astrophys. **549**, A106 (2013)
[19] D. Brown et al., Nucl. Data Sheets **148**, 1 (2018)